Research Article | Vol. 26, No. 23 | 12 Nov 2018 | OPTICS EXPRESS 30021
Optics EXPRESS

Tunable single-mode lasing in a single semiconductor microrod

YUE YANG,[1,4] TIANTIAN WEI,[1,4] RUI ZHU,[2] HUA ZONG,[1] JUNFENG LU,[3] JUNCHAO LI,[1] HUI LIAO,[1] GUO YU,[1] CAOFENG PAN,[3,5] AND XIAODONG HU[1,6]

[1]*State Key Laboratory for Artificial Microstructure and Mesoscopic Physics, School of Physics, Peking University, Beijing 100871, China*
[2]*Electron Microscopy Laboratory, School of Physics, Peking University, Beijing 100871, China*
[3]*Beijing Institute of Nanoenergy and Nanosystems, Chinese Academy of Sciences, Beijing 100083, China*
[4]*These authors contributed equally to this work*
[5]*cfpan@binn.cas.cn*
[6]*huxd@pku.edu.cn*

Abstract: Developing micro/nanoscale wire lasers with single-mode operation and lasing wavelength modulation is essential for realizing their practical applications such as optical communication and saturated spectroscopy. We demonstrated, to the best of our knowledge, the first tunable single-mode microrod laser without complicated micro/nano-manipulation and without additional environmental requirement. In this letter, we realized the wavelength modulation in a single semiconductor microrod simply and directly by changing the axial location of the active region, owing that the active region position plays a key role in determining the lasing mode of microrod lasers. Based on this feature, we proposed a pair of asymmetrical distributed Bragg reflectors (DBRs) with specific spectral selectivity to be induced in a GaN microrod to realize tunable single-mode lasing in a single semiconductor microrod. By using this method, lasing wavelength can be modulated from 369.5 to 375.7 nm flexibly and repeatedly in a 45 μm GaN microrod with the change of the excitation source position. This approach demonstrates a big application potential in numerous fields consisting of optical telecommunication and environmental monitoring.

1. Introduction

Semiconductor micro/nanoscale wire lasers, with one-dimensional structures, strong optical confinement, and sufficient optical gain, have been a hot issue of significant scientific research recently [1–5]. They are desirable modules for integratable micro/nanoscale coherent light sources for wide applications including sensing, digitized communications, and signal processing [6–9]. The spectrum purity of the microrod laser becomes an important figure of merit since laser emission at multiple frequencies can lead to temporal pulse broadening and high bit error ratio (BTR) because of group velocity dispersion [10]. Moreover, wavelength continuously variable lasers are required to satisfy the special needs in certain fields, such as optical communication and saturated spectroscopy [11,12].

Extensive researches have been done to modulate the lasing wavelength on a single wire or control microrod lasers to oscillate at a single frequency. In order to modulate the lasing wavelength on a single rod, cutting off the narrow-bandgap end section by section on a synthesized bandgap-graded rod is presented [13,14]. Sheng Liu, et al. has demonstrated controlled, continuous, and reversible wavelength tuning of single GaN nanowire laser by applying a hydrostatic pressure [15]. Besides, the multi-scattering effect at morphology defect sites of the nanoribbon, the absorption–emission–absorption process and Burstein–Moss effect have been utilized to tailor wavelength on a single nanorod [16–18]. To control

#341097 https://doi.org/10.1364/OE.26.030021
Journal © 2018 Received 31 Jul 2018; revised 21 Sep 2018; accepted 27 Sep 2018; published 31 Oct 2018

Optics EXPRESS

microrod lasers to oscillate at a single frequency, a variety of research methods are used, such as greatly shortening the lasing cavity path with expanded free space range (FSR) of the multiple longitude modes [19], and making use of coupled cavities, which can generate a mode selection mechanism by the Vernier effect [20–22]. However, to the best of our knowledge, there is not a way to achieve both wavelength modulation and single-mode lasing on a single microrod designed for the purpose of satisfying the requirements for modern optics and optoelectronics. In this letter, we demonstrate a GaN microrod laser that tailors the lasing wavelength as well as achieves the single-mode lasing.

To realize wavelength modulation repeatedly on a single microrod without modifying the geometry of resonant cavity or cutting the wire, our group have proposed the position-dependent lasing mechanism in GaN microrods that can tune the lasing wavelength over the broad band-edge emission of GaN (about 15 nm) [23]. Moreover, we have synthesized a GaN/InGaN core–shell structure that decouples the gain medium and optical cavity which modulates the lasing wavelength in a larger range (about 30 nm) flexibly and repeatedly on a single microrod [24].

2. Experiments and simulations

Based on our research and previous work experience, hybrid integration of distributed Bragg reflector (DBR) lasers is considered a promising approach to realize tunable single-mode lasing in a single semiconductor microrod to satisfy the requirements for modern optics and optoelectronics. By use of deep-etched grooves to form semiconductor–air DBRs, a short high-reflectivity reflector can be achieved with only a few periods. Although semiconductor/air DBR mirror has several advantages, high-contrast DBRs have poor spectral selectivity. Hence, a novel laser design with high performance and spectral selectivity is highly desirable. We use GaN as the semiconductor material. One of the main parameters for lasers is the differential gain (dg/dn), which ultimately determines the threshold current and other dynamic characteristics of a laser. Since better optical waveguiding can be obtained in GaN, the differential modal gain in GaN could then exceed that in unstrained GaInP, which shows that GaN is a promising material for laser. In this letter, a pair of asymmetrical DBRs with specific spectral selectivity was proposed and introduced to a GaN microrod to realize tunable single-mode lasing.

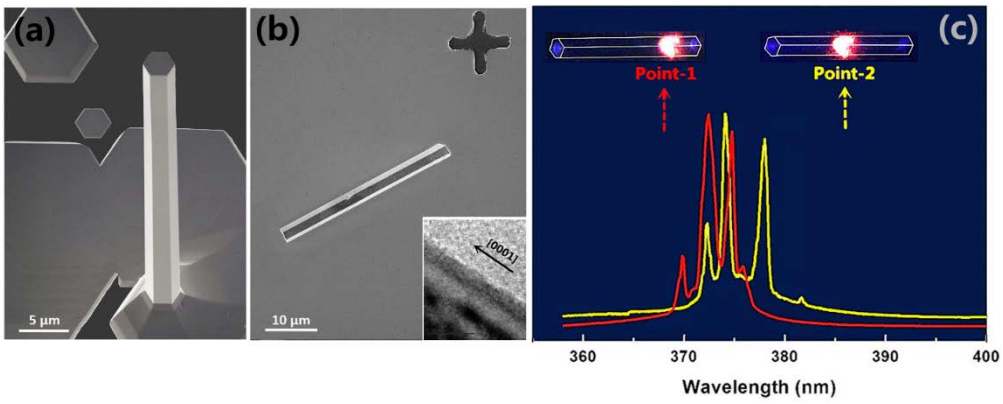

Fig. 1. (a) The SEM image of a single GaN microrod. (b) The SEM of a GaN microrod transferred to a marked Si substrate. Inset: The TEM micrograph of an individual GaN microrod. (c) Lasing spectrum of a single 45-μm-long, 3.8-μm-diameter GaN microrod pumped well above the lasing threshold at room temperature at different excitation positions.

The GaN microrods we used here were synthesized on sapphire substrates by Thomas Swan CCS-Metal Organic Chemical Vapor Deposition (MOCVD) system, using the same

Optics EXPRESS

fabrication process previously described in detail [23]. A typical scanning electron microscope (SEM) image of the microrod is displayed in Fig. 1(a), showing that the microrods have sharp cleaved end facets, with a hexagonal cross section. Figure 1(b) shows the SEM of a GaN microrod transferred to a marked Si substrate, indicating both facets of the microrod are relatively flat and smooth. Transmission electron microscopy (TEM) examinations demonstrate that the microrods are high-quality single crystal with growth along the [0001] direction (inset, Fig. 1(b)). The uniform thickness and smooth surface morphology of microrods are important for waveguiding without large losses from surface emission.

The room-temperature photoluminescence (PL) was inspected under the excitation of a He-Cd laser. The third harmonic (355 nm) of an Nd:YAG laser (1 kHz, 1 ns pulse width) was used as the excitation source. The approximate spot size of the laser is about 15 μm. The type of the spectrometer is Andor/SR-500i-D1-R, with a resolution of 0.08 nm. Lasing spectra of a single 45-μm-long, 3.8-μm-diameter GaN microrod are performed in Fig. 1(c). When the distance between the excitation source and the left end facet of the microrod changes from 35.2 μm (point-1) to 22.9 μm (point-2), the output laser mode exhibits an obvious change under the same pump power density that is demonstrated in Fig. 1(c). The insets above the spectrum is the corresponding charge-coupled device (CCD) image of optical emission from the GaN microrod. Changing the axial location of the active region directly leads to the variation of the field interference between the dipole sources and two end facets of the microrod and therefore modifies the dipole strength as well as the field distribution in microrods, consequently altering the lasing mode. This phenomenon has been explained in detail in our previous work [23]. The position of the active region plays a key role in determining the lasing mode of microrod lasers, which can be used to realize microrod laser modulation simply and directly. From Fig. 1(c) we can see that, although lasing wavelength can be tuned in a GaN microrod repeatedly, multi-mode lasing making these tunable microrod lasers difficult to apply in practical applications such as saturated spectroscopy, environmental monitoring and optical communication.

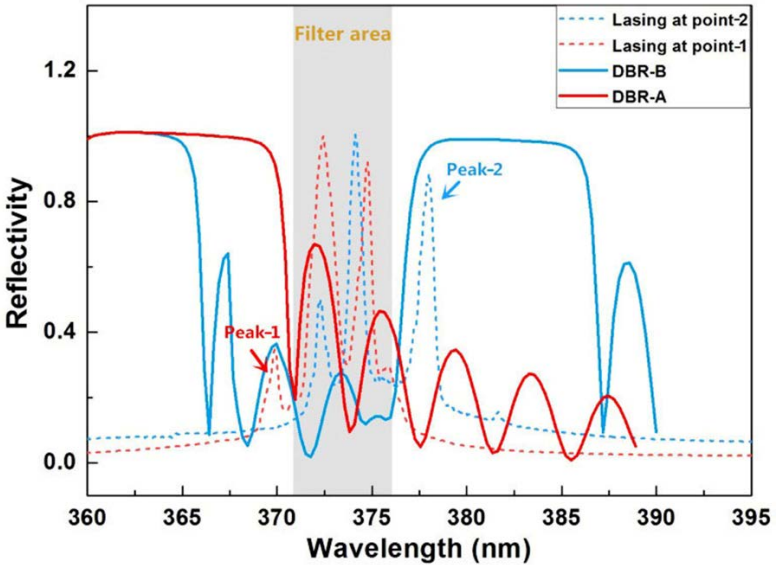

Fig. 2. The normalized reflection spectra of DBR-A and DBR-B.

Combined our research and based on previous work experience, we propose a pair of asymmetrical DBR with specific spectral selectivity to be introduced in a GaN microrod to

Optics EXPRESS

realize tunable single-mode lasing in a single semiconductor microrod. Numerical simulations based on 3D finite difference time-domain (FDTD) method were used to guide the design of the DBR geometry and to analyze the results from the experimental measurements. Here the simulations were calculated by 3D FDTD solutions tools (Lumerical FDTD Solutions, Inc.). We set the length and the diameter of the simulated GaN microrod to be 45 μm and 3.8 μm respectively, which is same with the size of the microrod sample analyzed in Fig. 1(c). The wavelength-dependent refractive index of GaN based on experimental measurements is taken from Ref [25]. The fundamental mode was injected and propagated through the microrod. Everything is enclosed by perfectly matched layers (PMLs) that absorb any radiation impinging on the domain boundaries. The complex reflection coefficients are extracted by monitoring the wave's propagation through the structure.

A pair of DBRs called DBR-A and DBR-B is designed to be integrated at two ends of the wire cavity, respectively. The optical properties of DBR-A and DBR-B in the GaN microrod were investigated from 3D FDTD simulations, and these simulations were used to predict the position of the stopband and therefore guide the design of the DBR geometry. Bragg condition from coupled mode theory is presented for better understanding of the optimization design [26,27]: $m\lambda_B = 2n_{eff}\Lambda$, where m is the order, λ_B is the Bragg wavelength, n_{eff} is the effective refractive index, and Λ is the grating parameter. The grating parameters to be optimized in our simulation are the etch width (W), the etch depth (ΔW), the number of periods (N), the grating period (L), and $D = W / L$ represents the duty cycle. It was found in the simulation that the position of the stopband and the full-width at half-maximum (FWHM) of these bands are more sensitive to the duty cycle rather than the cut depth or the number of the periods. A deeper cut depth or wider cut width will lower the effective index of refraction and therefore blue shift the stopband slightly. Different from other regular gratings that are relatively long with a large number of periods, we carefully designed the DBRs to be as short as possible to reduce the influence of ion etch on the cavity length and avoid the change of the laser spectrum shown in Fig. 1(c). The grating parameters of DBR-A /DBR-B have been carefully designed through the FDTD method as follows: the etching width W = 32 /26 nm, the grating period L = 700 /800 nm and the number of the periods N = 4 /4. The groove depth of both DBRs is 2 μm.

The normalized reflection spectra of the two DBRs are shown in Fig. 2. From the figure, we can see that the low-reflection areas of two DBRs are different but interlaced. The purpose of such design is twofold: The first is that the overlap region of the low-reflection areas of DBR-A and DBR-B is carefully designed to filter the multiple lasing modes of the microrod laser, which is indicated by the grey region and is defined as the "Filter area". The second is that the high-reflection areas, namely the forbidden bands, are designed to match the selected lasing wavelengths which are expected to be preferentially excited. In our experiments, resonant wavelength varies with the change of the active region where wavelength tunability can be realized by altering the pumping region. Two lasing wavelengths at 369.8 nm (marked as "peak-1", Fig. 2) and at 378.1 nm (marked as "peak-2", Fig. 2) are selected as the specifically tuned resonant wavelengths on a single microrod laser. Combined the PL experiments (Fig. 1(c)) with the reflectivity of the designed asymmetrical DBRs (Fig. 2), it is predictable that when the pumping source locates at point-1, only lasing mode at 369.8 nm (peak-1) is in the forbidden band of DBR-A which has priority to be excited. Meanwhile, the other lasing modes are in the filter area and less competitive than the lasing mode in the forbidden band. Based on these two reasons, there is a high possibility that only the lasing wavelength in the forbidden band, namely peak-1, is excited when the pumping source locates at point-1. Similarly, when the excitation source locates at point-2, lasing wavelength at 378.1 nm (peak-2), which is in the forbidden band of DBR-B will be preferentially excited with the other lasing modes in the filter area. Therefore, by changing the excitation position in a microrod, tunable single-mode lasing is expected to be realized at specific resonant

Optics EXPRESS

wavelength with the use of asymmetrical DBRs, where the length of the tuning lasing wavelength is about 8.3 nm.

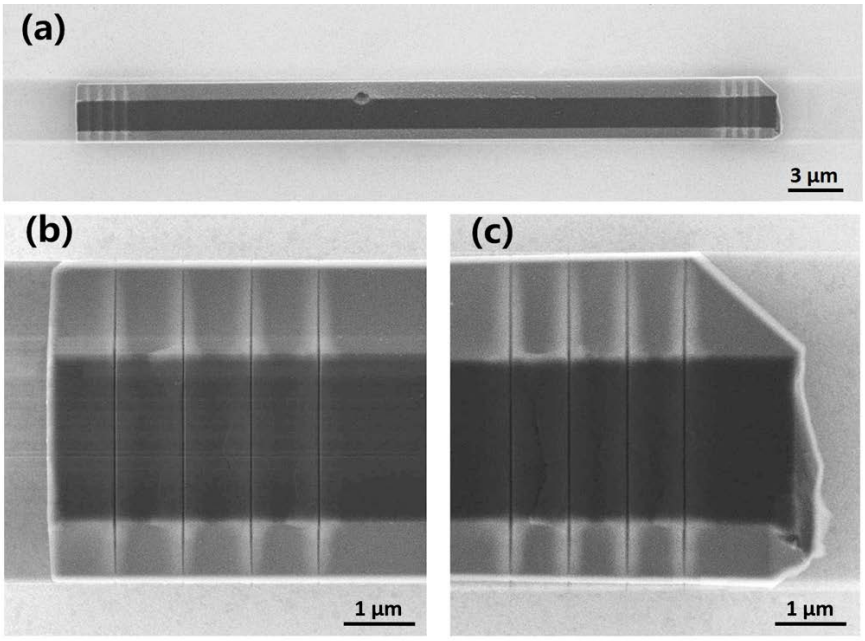

Fig. 3. The helium ion microscope image of the 45-μm-long, 3.8-μm-diameter GaN microrod after fabricating DBRs. The image of (a) the whole wire cavity, (b) the left end of the cavity integrated with DBR-B and (c) the right end of the cavity integrated with DBR-A.

DBRs were carefully fabricated according to the guidelines of the simulation presented. A ZEISS ORION NanoFab helium ion microscope was used to pattern periodic indentations into microrods by 30 kV focused helium ion beam with controlled periodicity, duty cycle, and depth. Four periodic gratings were etched off at the left end of the cavity with 26-nm wide slits, and 800-nm sized intervals while at the right end of the cavity with 32-nm wide slits and 700-nm sized intervals by the focused helium ion etching process, which is shown in Fig. 3. The dose of 11.35 nC/μm^2 and beam current of 5.6 pA were used for grating fabrications. The groove depth was carefully controlled to about 200 nm, as deeper grooves etched at higher doses would be accompanied with more ion injecting damages to the fabricated structures.

Optics EXPRESS

3. Experimental results and discussion

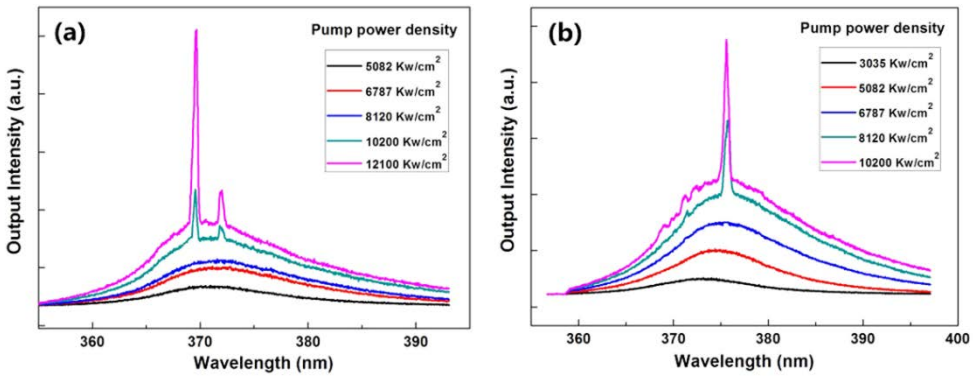

Fig. 4. The laser spectrum of the 45-μm-long, 3.8-μm-diameter GaN microrod with integrated DBRs at room temperature when the pumping source locates at (a) point-1 and (b) point-2.

In the experiment on laser excitation for the 45-μm-long, 3.8-μm-diameter GaN microrod with integrated DBRs at room temperature, as shown in Fig. 4, the excited point changes from point-1 to point-2. We collect the complete emission from the microrod rather than one end face of it. Figure 4(a) shows the laser spectrum of the GaN microrod after fabricating DBRs when the excitation light spot locates at point-1. With a pump intensity of 12100 kW/cm^2, the resonant mode at a wavelength of 369.5 nm shows a good single-mode behavior, with the calculated side-mode suppression ratio (SMSR) to be 8.5 dB and FWHM to be approximately 0.5 nm. When the position of the excitation light spot changes from point-1 to point-2, as illustrated in Fig. 4(b), the lasing wavelength of the GaN microrod with integrated DBRs changes to 375.7 nm, which demonstrates better monochromaticity and shows a single sharp peak with a FWHM of 0.8 nm. Moreover, from Fig. 4 we can see that the microrod laser exhibits stable single-frequency operation under two excitation conditions over a range of pump power densities above the threshold. We can see the FWHM values of the lasing modes are quite large, which can be attributed to the large diameter of the microrod. Since the microrod has large size with a diameter of 3.8 μm, there is almost no confinement to the transverse light field and there are no more restriction measures for the light field, therefore the linewidths of the lasing modes from the 3.8-μm-diameter microrod are a little large.

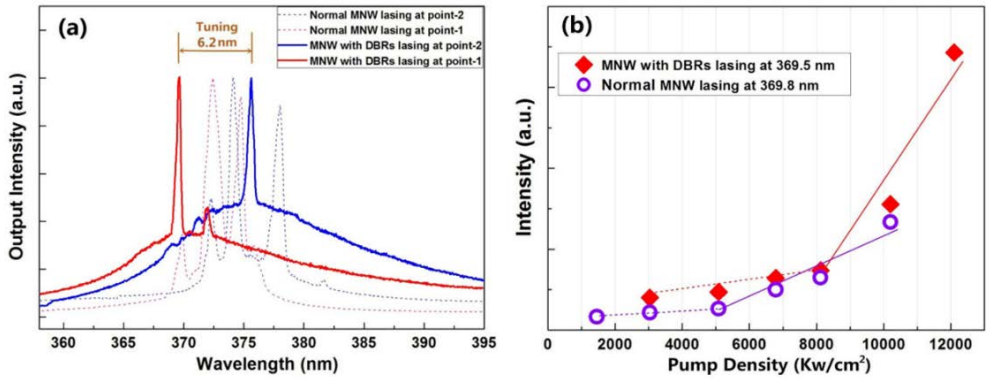

Fig. 5. (a) Lasing spectrum and (b) laser power dependence of the 45-μm-long, 3.8-μm-diameter GaN microrod with and without the designed asymmetrical DBRs.

Optics EXPRESS

To take a comprehensive view of the experiment results, we compare the lasing spectrum of the 45-μm-long, 3.8-μm-diameter GaN microrod with and without the designed asymmetrical DBRs in Fig. 5(a). Before integrated with DBRs, the wire laser exhibits multiple-mode emission with several remarkable peaks. As the lasing wavelength changes with the position change of the excitation source, we designed a pair of asymmetrical DBR integrated in the GaN microrod to realize tunable single-mode lasing by means of merely changing the position of the pumping region. Under the envisaged plans, the specific lasing wavelength is supposed to be tuned from 369.8 nm (marked as "peak-1", Fig. 2) to 378.1 nm (marked as "peak-2", Fig. 2). After fabricating DBRs in the GaN microrod, we can get different single-mode lasing wavelengths at different excitation point, and the lasing wavelength is tuned from 369.5 to 375.7 nm with the position of the excitation light spot changing from point-1 to point-2. So far, we have successfully realized tunable single-mode lasing in a single semiconductor microrod with the use of asymmetrical DBRs. However, the lasing wavelength is not the same as what we accurately designed. For future improvement of the accuracy of the experiment and better use of the asymmetrical DBRs design, the causes that may induce the deviation of the lasing wavelength from the designed value are analyzed. Firstly, although the synthesized GaN microrod has sharp cleaved end facet which is flat and smooth as Fig. 1(a) shows, the bottom of the microrod is chipped when a GaN microrod is transferred to a marked Si substrate, indicating one end facet of the microrod is not so flat which is shown in Fig. 3(c). In the helium ion beam etching process, we avoid and reserve the uneven area of the chipped end facet, which leads DBR-A to be longer than what we designed and that has been illustrated in Fig. 3(c). An efficient way to address this issue is to smooth the chipped end facet of the microrod by means of ion beam etching, before we select the specific lasing wavelength and design the asymmetrical DBRs. Secondly, the grating parameters of DBR-A /DBR-B are designed as follows: the etching width W = 32 /26nm, the grating period L = 700 /800 nm and the number of the periods N = 4 /4. Hence, the required total DBR length is about 6.2 μm. The GaN microrod is 45 μm long, that is to say, the resonant cavity of the lasing modes resonated between two microrod -end facets is 45 μm. After fabricating the 6.2-μm-long DBRs in the GaN microrod, the resonant cavity of the lasing modes decreases from 45 μm to about 38.8 μm, leading to the change of the lasing mode in the microrod laser [28,29]. An effective means to address this issue is to fabricate external DBRs outside the resonant cavity to eliminate the effect of the resonant cavity length reduction.

The laser power dependence measured at point-1 with and without the designed asymmetrical DBRs is shown in Fig. 5(b). The feature of the power dependence measured at point-2 with and without the designed asymmetrical DBRs is similar. From this figure we can see that the excitation thresholds under multi-mode lasing (6787 kW/cm^2) is lower than that under single-mode lasing (8120 kW/cm^2) when the laser is excited at the same position. This phenomenon can be caused by several complex factors. In lasers, the threshold condition is defined as the point at which the round-trip gain inside a cavity balanced by the round-trip loss, that can be illustrated in the following equations [30,31]:

$$\frac{L_g}{L}\Gamma g_{th} = \alpha_p + \alpha_m \tag{1}$$

$$\alpha_m = \frac{1}{2L}\ln\frac{1}{R_1 R_2} \tag{2}$$

where Γ is the confinement factor, g_{th} is the threshold gain, L is the length of the semiconductor rod, L_g is the length of the gain region, α_m is the mirror loss, α_p is the propagation loss, and R_1 and R_2 are the reflection coefficients for each end facet. Γ for 369.5

Optics EXPRESS

nm is almost equal to Γ for 369.8 nm. L and L_g for both wavelengths are also the same. Ion beam etching brings the interface scattering loss when waveguides propagate in the cavity, and therefore α_p for 369.5 nm is larger than that for 369.8 nm [32]. On the other hand, although the simulation demonstrates that the reflectivity of the two end faces of GaN cavity with integrated DBR mirrors can reach up to 0.9, the actual reflectivity of the two end faces will be much smaller than 0.9. The reasons are as follows. Since the great contrast between the narrow etching width and the large diameter of the GaN microrod brings a great deal of difficulty and complexity to ion beam etching, the actual cut depth of DBRs will be much shorter than what we designed. Hence, the actual reflectivity of the two end faces is also much smaller than the design value. Therefore, although α_m for 369.5 nm is smaller than that for 369.8 nm, α_p for 369.5 nm is much larger than that for 369.8 nm, leading $\alpha_p + \alpha_m$ as a whole for 369.5 nm bigger than that for 369.8 nm. These integrated factors make g_{th} for 369.5 nm higher than g_{th} for 408 nm, which is consistent with the experimental result (Fig. 5(b)). A simple way to reduce the lasing threshold of microrod lasers with integrated DBRs is to reduce the diameter of the synthesized semiconductor microrod. In this way, with the difficulty of etching decreases and cut depth of DBRs increases, the reflectivity of the two end faces of microrods will be greatly improved and therefore the lasing threshold can be significantly reduced.

4. Summary

In summary, we firstly proposed a pair of asymmetrical DBRs with specific spectral selectivity to be induced in a GaN microrod to realize tunable single-mode lasing in a single semiconductor microrod. The overlap region of the low-reflection areas of two DBRs was carefully designed to filter the multiple lasing modes of the microrod laser, meanwhile, the high-reflection areas were designed to match the selected lasing wavelengths which are expected to be preferentially excited. After fabricating DBRs in the GaN microrod, an obvious transition from multiple-mode emission to single-mode emission of the microrod is observed. By using this method, lasing wavelength can be modulated from 369.5 to 375.7 nm flexibly and repeatedly in a 45-μm-long, 3.8-μm-diameter GaN microrod with the change of the position of the excitation source. Although there are some deviations of the experimental results from the design intent, corresponding improved measures were put forward on the basis of reason analysis for future improvement of the experiment accuracy and better use of the design concept. This idea of tunable single-mode microrod lasers structural design can be applied in many material systems, which demonstrates a big application potential in numerous fields consisting of optical telecommunication and environmental monitoring.

Funding

Science Challenge Project (TZ2016003-2-106); Key National Research and Development Program (2017YFB0405000); National Natural Science Foundation of China (NSFC) (61334005); Beijing Municipal Science and Technology Project, China (Z61100002116037).

Acknowledgments

The authors would like to thank all the staff during the measurements at the beamline 1W1A at BSRF.

References

1. R. Chen, T.-T. D. Tran, K. W. Ng, W. S. Ko, L. C. Chuang, F. G. Sedgwick, and C. Chang-Hasnain, "Nanolasers grown on silicon," Nat. Photonics **5**(3), 170–175 (2011).
2. C. J. Barrelet, J. Bao, M. Loncar, H.-G. Park, F. Capasso, and C. M. Lieber, "Hybrid single-nanowire photonic crystal and microresonator structures," Nano Lett. **6**(1), 11–15 (2006).
3. R. Yan, D. Gargas, and P. Yang, "Nanowire photonics," Nat. Photonics **3**(10), 569–576 (2009).

Optics EXPRESS

4. C. Li, J. B. Wright, S. Liu, P. Lu, J. J. Figiel, B. Leung, W. W. Chow, I. Brener, D. D. Koleske, T.-S. Luk, D. F. Feezell, S. R. J. Brueck, and G. T. Wang, "Nonpolar InGaN/GaN core–shell single nanowire lasers," Nano Lett. **17**(2), 1049–1055 (2017).
5. H. Zhu, Y. Fu, F. Meng, X. Wu, Z. Gong, Q. Ding, M. V. Gustafsson, M. T. Trinh, S. Jin, and X.-Y. Zhu, "Lead halide perovskite nanowire lasers with low lasing thresholds and high quality factors," Nat. Mater. **14**(6), 636–642 (2015).
6. M. Zapf, R. Röder, K. Winkler, L. Kaden, J. Greil, M. Wille, M. Grundmann, R. Schmidt-Grund, A. Lugstein, and C. Ronning, "Dynamical Tuning of Nanowire Lasing Spectra," Nano Lett. **17**(11), 6637–6643 (2017).
7. A. B. Vasista, H. Jog, T. Heilpern, M. E. Sykes, S. Tiwari, D. K. Sharma, S. K. Chaubey, G. P. Wiederrecht, S. K. Gray, and G. V. P. Kumar, "Differential Wavevector Distribution of Surface-Enhanced Raman Scattering and Fluorescence in a Film-Coupled Plasmonic Nanowire Cavity," Nano Lett. **18**(1), 650–655 (2018).
8. M. Spies, M. I. den Hertog, P. Hille, J. Schörmann, J. Polaczyński, B. Gayral, M. Eickhoff, E. Monroy, and J. Lähnemann, "Bias-controlled spectral response in GaN/AlN single-nanowire ultraviolet photodetectors," Nano Lett. **17**(7), 4231–4239 (2017).
9. Y. Xia, P. Yang, Y. Sun, Y. Wu, B. Mayers, B. Gates, Y. Yin, F. Kim, and H. Yan, "One-dimensional nanostructures: synthesis, characterization, and applications," Adv. Mater. **15**(5), 353–389 (2003).
10. B. E. A. Saleh and M. C. Teich, *Fundamentals of Photonics* (Wiley, 2007), Chapter 14.
11. T. W. Hänsch, I. S. Shahin, and A. L. Schawlow, "High-Resolution Saturation Spectroscopy of the Sodium D Lines with a Pulsed Tunable Dye Laser," Phys. Rev. Lett. **27**(11), 707–710 (1971).
12. J. Buus and E. J. Murphy, "Tunable lasers in optical networks," J. Lightwave Technol. **24**(1), 5–11 (2006).
13. J. Xu, X. Zhuang, P. Guo, W. Huang, W. Hu, Q. Zhang, Q. Wan, X. Zhu, Z. Yang, L. Tong, X. Duan, and A. Pan, "Asymmetric light propagation in composition-graded semiconductor nanowires," Sci. Rep. **2**(1), 820 (2012).
14. Z. Yang, D. Wang, C. Meng, Z. Wu, Y. Wang, Y. Ma, L. Dai, X. Liu, T. Hasan, X. Liu, and Q. Yang, "Broadly defining lasing wavelengths in single bandgap-graded semiconductor nanowires," Nano Lett. **14**(6), 3153–3159 (2014).
15. S. Liu, C. Li, J. J. Figiel, S. R. J. Brueck, I. Brener, and G. T. Wang, "Continuous and dynamic spectral tuning of single nanowire lasers with subnanometer resolution using hydrostatic pressure," Nanoscale **7**(21), 9581–9588 (2015).
16. X. Liu, Q. Zhang, Q. Xiong, and T. C. Sum, "Tailoring the lasing modes in semiconductor nanowire cavities using intrinsic self-absorption," Nano Lett. **13**(3), 1080–1085 (2013).
17. J. Li, C. Meng, Y. Liu, X. Wu, Y. Lu, Y. Ye, L. Dai, L. Tong, X. Liu, and Q. Yang, "Wavelength Tunable CdSe Nanowire Lasers Based on the Absorption-Emission-Absorption Process," Adv. Mater. **25**(6), 833–837 (2013).
18. Y. Lu, F. Gu, C. Meng, H. Yu, Y. Ma, W. Fang, and L. Tong, "Multicolour laser from a single bandgap-graded CdSSe alloy nanoribbon," Opt. Express **21**(19), 22314–22319 (2013).
19. Q. Li, J. B. Wright, W. W. Chow, T. S. Luk, I. Brener, L. F. Lester, and G. T. Wang, "Single-mode GaN nanowire lasers," Opt. Express **20**(16), 17873–17879 (2012).
20. Y. Xiao, C. Meng, P. Wang, Y. Ye, H. Yu, S. Wang, F. Gu, L. Dai, and L. Tong, "Single-nanowire single-mode laser," Nano Lett. **11**(3), 1122–1126 (2011).
21. H. Gao, A. Fu, S. C. Andrews, and P. Yang, "Cleaved-coupled nanowire lasers," Proc. Natl. Acad. Sci. U.S.A. **110**(3), 865–869 (2013).
22. Y. Xiao, C. Meng, X. Wu, and L. Tong, "Single mode lasing in coupled nanowires," Appl. Phys. Lett. **99**(2), 023109 (2011).
23. Y. Yang, H. Zong, C. Ma, T. Wei, J. Li, J. Zhang, M. Li, C. Pan, and X. Hu, "Self-selection mechanism of Fabry-Pérot micro/nanoscale wire cavity for single-mode lasing," Opt. Express **25**(18), 21025–21036 (2017).
24. H. Zong, Y. Yang, C. Ma, X. Feng, T. Wei, W. Yang, J. Li, J. Li, L. You, J. Zhang, M. Li, C. Pan, X. Hu, and B. Shen, "Flexibly and Repeatedly Modulating Lasing Wavelengths in a Single Core-Shell Semiconductor Microrod," ACS Nano **11**(6), 5808–5814 (2017).
25. M. M. Y. Leung, A. B. Djurišić, and E. H. Li, "Refractive index of InGaN/GaN quantum well," J. Appl. Phys. **84**(11), 6312–6317 (1998).
26. R. Su, C. Diederichs, J. Wang, T. C. H. Liew, J. Zhao, S. Liu, W. Xu, Z. Chen, and Q. Xiong, "Room-temperature polariton lasing in all-inorganic perovskite nanoplatelets," Nano Lett. **17**(6), 3982–3988 (2017).
27. A. Fu, H. Gao, P. Petrov, and P. Yang, "Widely Tunable Distributed Bragg Reflectors Integrated into Nanowire Waveguides," Nano Lett. **15**(10), 6909–6913 (2015).
28. L. Chen and E. Towe, "Coupled optoelectronic modeling and simulation of nanowire lasers," J. Appl. Phys. **100**(4), 44305 (2006).
29. A. Dodabalapur, L. J. Rothberg, R. H. Jordan, T. M. Miller, R. E. Slusher, and J. M. Phillips, "Physics and applications of organic microcavity light emitting diodes," J. Appl. Phys. **80**(12), 6954–6964 (1996).
30. S. Arafin, X. Liu, and Z. Mi, "Review of recent progress of III-nitride nanowire lasers," J. Nanophotonics **7**(1), 074599 (2013).
31. A. B. Djurisić and Y. H. Leung, "Optical properties of ZnO nanostructures," Small **2**(8-9), 944–961 (2006).
32. P. Roberts, F. Couny, H. Sabert, B. Mangan, T. Birks, J. Knight, and P. Russell, "Loss in solid-core photonic crystal fibers due to interface roughness scattering," Opt. Express **13**(20), 7779–7793 (2005).